JOURNAL OF MATERIALS SCIENCE 19 (1984) 983–999

Short silk fibre reinforced nitrile rubber composites

D. K. SETUA, S. K. DE
Rubber Technology Centre, Indian Institute of Technology, Kharagpur 721302, India

The role of "resorcinol–hexamethylenetetramine–silica" bonding system in adhesion between silk fibre and nitrile rubber has been studied. Definite proportions of the three components of the bonding system *vis-à-vis* fibre loading are found to provide the optimum set of technical properties. Increase of fibre concentration in the composites causes an increase in hardness, tensile strength, tear strength, modulus, heat build-up, compression set at constant strain, abrasion loss, and restriction to solvent-swelling and a simultaneous decrease in some properties like resilience, compression set at constant stress and elongation at break. Ageing enhances the adhesion level and shows improved retention of strength properties of the composites. Increasing fibre loading in the mixes leads to a significant improvement in processing characteristics. Scanning electron microscopy studies of fracture surfaces obtained from tensile, tear, abrasion and heat build-up testing have been made in order to assess the failure mode.

1. Introduction

Short fibre-reinforced rubber composites have become very propular nowadays because of their processing advantages and good technical properties like strength, stiffness, elastic modulus, creep rate, damping, etc. [1–7]. Recently, Setua and De [1] have reported results of their studies on short silk fibre-reinforced natural rubber composites. Studies have also been made earlier on the utilization of jute fibre as a reinforcing filler in natural rubber (NR) [8], styrene–butadiene rubber (SBR) [9] and carboxylated nitrile rubber (XNBR) [10]. The role of the "resorcinol–hexamethylenetetramine–silica" bonding system to promote adhesion between fibres and rubbers has also been reported [11–13]. The composite properties have been found to depend very much on the extent of adhesion between the fibre and the rubber matrix and also on factors like fibre concentration, orientation, dispersion and aspect ratio (length to diameter ratio).

Silk fibre, because of the presence of many functional groups like $-NH_2$, $-COOH$, $-NHCO$, $-CH_2OH$ on its surface, is polar in nature. This fibre has got a non-cellular structure in contrast to other natural fibres like jute and cotton. Nitrile rubber too is a polar rubber due to the acrylonitrile group. The above characteristics of the fibre and the rubber are expected to produce excellent adhesion/bonding between the silk fibre and the nitrile rubber in their composites.

The importance of short fibre reinforcement in the production of hoses, V-belts and in the manufacture of complex shaped mechanical goods have been studied by many workers [14–17]. The feasibility of using short fibre-reinforced nitrile rubber for the production of high performance automotive fuel hoses has been reported by Horvath [18].

We report in this paper the results of our studies on silk fibre-reinforced nitrile rubber composites. We have used waste silk fibre obtained during cocoon reeling which is unusable as such in the textile industry. In this context, the present work deals with the utilization of a waste material in rubber.

The present studies can be divided into the following parts:

(i) effect of bonding agents, e.g. "resorcinol–hexamethylenetetramine (hexamine)–silica" concentration in achieving improved adhesion;

(ii) optimization of the requisite concentrations

0022–2461/84 $03.00 + .12

of bonding agents *vis-à-vis* fibre loading;

(iii) anisotropy in the technical properties of fibre–rubber composites;

(iv) ageing resistance of the composites and

(v) processing characteristics.

Scanning electron microscopy (SEM) studies of the fractured surfaces have also been made in order to understand the role of bonding agents in adhesion and the failure mechanism.

2. Experimental procedure

Waste silk fibre was first separated from undesirable foreign matter and chopped to 6 mm length. Mixing operation was carried out on a conventional laboratory open mill (150 mm x 330 mm) at 30–40° C according to ASTM designation D 15-70. Nitrile rubber because of its higher plasticity compared to natural rubber develops more heat when mixed under similar conditions. Plasticity was lowered by masticating on a cold tight mill for 5 minutes prior to the addition of other ingredients. Nip gap, mill roll speed ratio, time of mixing and the sequence of addition of the ingredients were kept same for all the mixes. Solubility of sulphur in nitrile rubber is much lower than in natural rubber. Therefore, sulphur was added to the mixes just after the addition of zinc oxide for better dispersion. Shear force during mixing oriented most of the fibres along the grain direction [1, 9, 10] but this also caused breakage of the fibres. Extent of fibre breakage was determined by dissolution of the compound in chloroform, followed by extraction of the fibres and examination of fibre length distribution by a polarizing microscope under reflected light (model Leitz HM-Pol).

A fall in the mean aspect ratio from its original value of 500 to 77 after mixing is almost the same for all the mixes. The breakage pattern of the fibres due to mixing is shown in Fig. 1. However, no change in average diameter (0.012 mm) occurred during mixing.

Optimum cure times at 150° C for the mixes were obtained by using Monsanto R-100 rheometer. Mixes were vulcanized to their respective cure times at 150° C and 4.5 N mm^{-2} pressure in a hydraulic press having electrically heated platens. The details of the preparation of vulcanizates have already been reported elsewhere [19]. Stress–strain properties were determined by using Instron Universal Testing Machine (Model 1195) at a crosshead speed of 500 mm per minute.

Both tensile and tear testing were done at 30° C

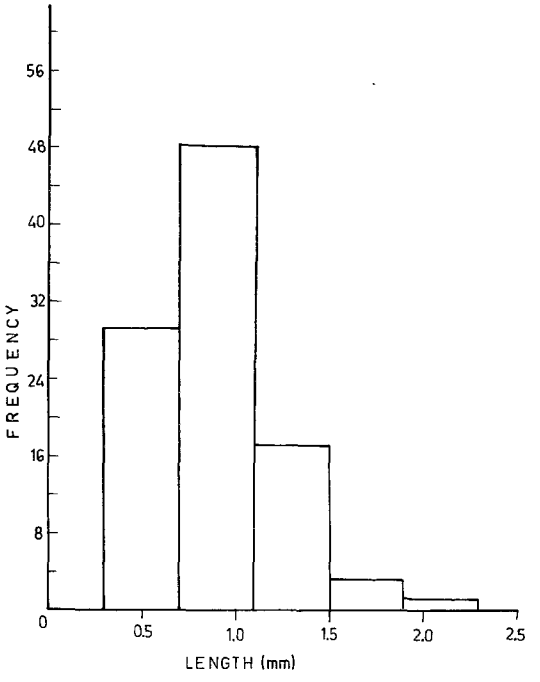

Figure 1 Distribution of length of broken fibres after mixing as obtained with the polarizing microscope.

according to ASTM methods D 412-51T and D 624-54. Shore A hardness was measured according to ASTM D 676-52T. Compression set at constant stress (400 lb) and the same at constant strain (25% strain) were measured according to ASTM methods D 395-61, method A and D 395-61, method B, respectively. Heat build-up measurements were done in a Goodrich flexometer as per ASTM D 623-67, method A. Resilience was determined at 35° C by using a Dunlop tripsometer according to BS 903 part-2 1950. Abrasion loss of the composites was measured by using the Du Pont abrader as per ASTM D 394, method A. The specimens were abraded for 10 min and the abrasion loss was calculated in terms of volume loss per hour. The wear behaviour of the composites was investigated under two directions of fibre-orientation with respect to the sliding direction of the abrasive disc of the abrader. Tests like tensile, tear, compression set, heat build-up were carried out both along (longitudinally oriented fibres) and across (transversely oriented fibres) the grain direction. Resilience and hardness measurements were made with tensile sheet specimens and orientation of the fibres in these cases was normal to the direction of the application of the load.

Figs. 2a and b show the shapes of the tensile and tear test specimens with longitudinally and

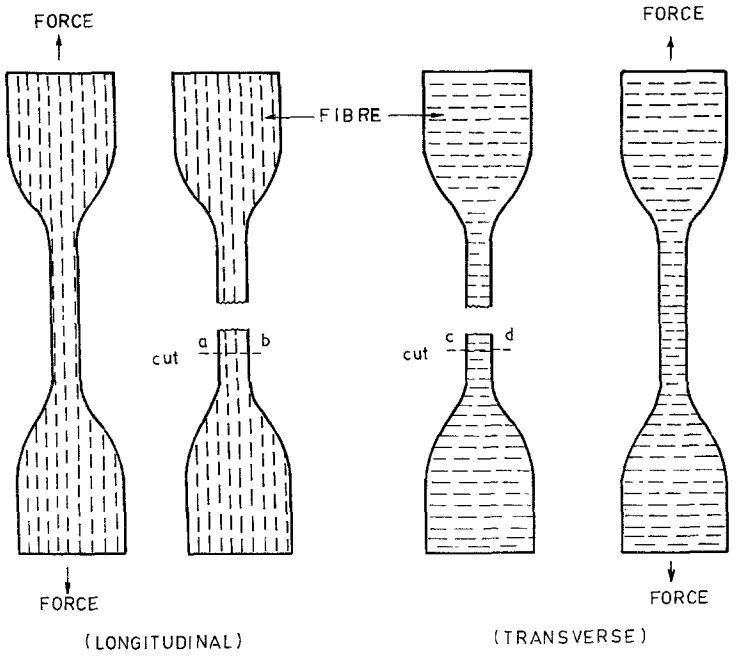

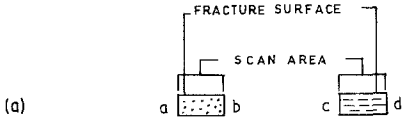

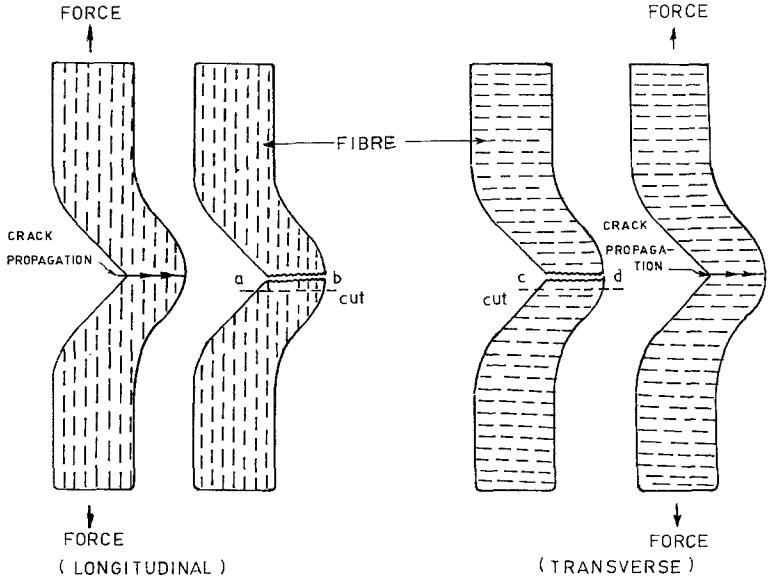

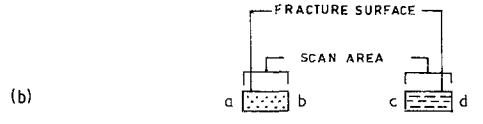

Figure 2 (a) Shapes of the tensile test specimens with longitudinal and transverse fibre orientation, corresponding fractured surfaces and scan areas. (b) Shapes of the tear test specimens with longitudinal and transverse fibre orientation, corresponding fractured surfaces and scan areas. (c) Fibre directionality and scan areas in the test specimens of abrasion and heat build-up tests. (d) Fibre directionality in the test specimens of compression set, resilience and hardness tests.

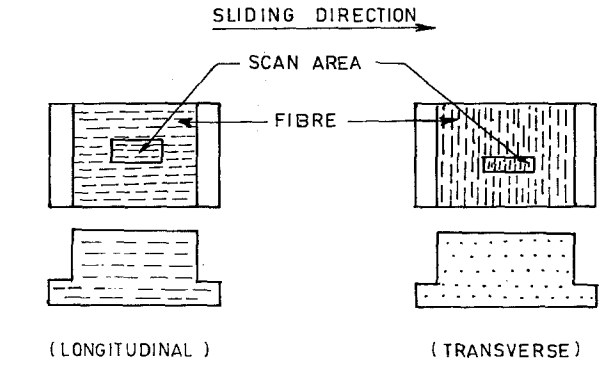

ABRASION TEST SPECIMENS

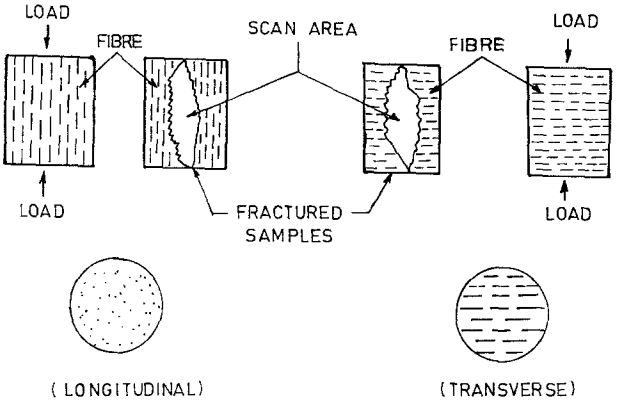

(c) HEAT BUILD-UP TEST SPECIMENS

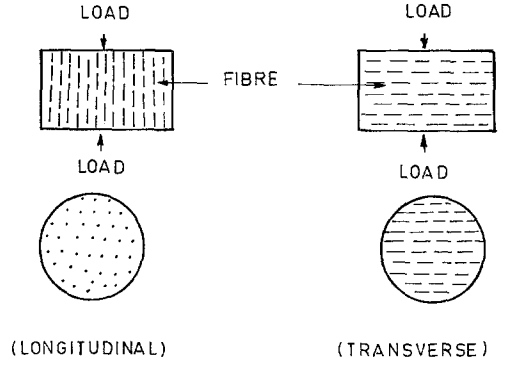

COMPRESSION SET TEST SPECIMENS

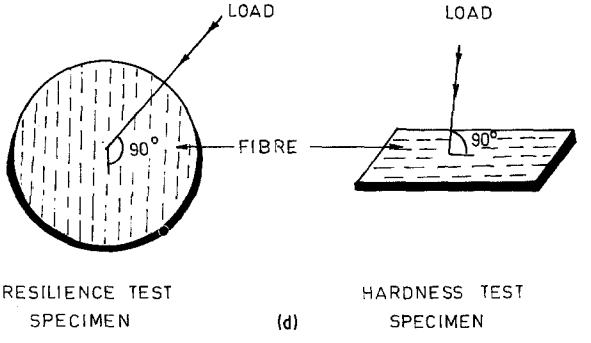

(d)

Figure 2 Continued.

transversely oriented fibres, and the corresponding fractured surfaces and scan areas. Fig. 2c shows the fibre directionality in the test specimens of abrasion and heat build-up tests. The portion of the specimen used for SEM studies have also been shown in the samples. The axes of the test geometry with reference to fibre directionality for compression set, resilience and hardness test samples are depicted in Fig. 2d. The fracture surfaces were sputter-coated with gold within 24 h of testing. SEM studies were carried out using a Philips model 500 scanning electron microscope. The orientation of the photographs was kept constant for a particular mode of testing and the tilt adjusted to 0° C for all samples.

Volume fraction of the rubber in the swollen vulcanizate (V_r), was calculated using the method suggested by Ellis and Welding [20, 21], which takes into account the correction of swelling increment with duration of immersion after the equilibrium is attained. Equilibrium was obtained after 48 h of swelling in chloroform at 35° C.

$$V_r = \frac{(D - FT)\,\rho_r^{-1}}{(D - FT)\,\rho_r^{-1} + A_0\rho_s^{-1}}$$

where T, the weight of the test specimens, D is the deswollen weight of the test specimens, F is the weight fraction of insoluble components, A_0 is the weight of the absorbed solvent, corrected for the swelling increment and ρ_r and ρ_s are the densities of the rubber and the solvent, respectively. $\rho_r = 0.98\,g\,cm^{-3}$ for NBR, and $\rho_s = 1.48\,g\,cm^{-3}$ for chloroform.

The tensile and tear specimens were aged for 48 h at 100° C in a Blue MFC 712 air oven to determine the retention of tensile strength, elongation at break and tear strength after ageing.

The green strength of the compounds was determined by the method of Foldi [22]. The compound was cured for 2 min at 121° C in order to remove tack and the stress at yield point was taken as the green strength. Mill shrinkage was determined according to ASTM method D 1917-62T. Mooney viscosity and Mooney scorch time were determined at 120° C as per ASTM procedure D 927-52T.

3. Results and discussion

3.1. Role of "resorcinol–hexamethylenetetramine–silica" in the adhesion/bonding between the fibre and the rubber

Formulations of the mixes and characterization of the vulcanizates are given in Tables I and II, respectively. Tear strength in both the orientations and hardness for the fibre filled mixes are higher than that for the mixes without fibre (e.g. mixes A and G). From the tensile strength values (Table II) it is evident that the gum strength of nitrile rubber (mix A) is very low. Addition of fibres (mixes B and C) improves tensile strength marginally while elongation at break values drop sharply. Tensile strength, elongation at break and modulus values of mix D (resorcinol–hexamine alone) and mix E (silica alone) are comparable to mixes containing fibre alone (mixes B and C). However, when resorcinol–hexamine–silica bonding system is present in the fibre–rubber mix (mix F), sharp increases are noted in tensile strength and modulus and in the anisotropy in elongation at break values.

TABLE I Formulations of the mixes A to G

Ingredient	Content of mix (parts by weight)						
	A	B	C	D	E	F	G
NBR*	100	100	100	100	100	100	100
Zinc oxide	5	5	5	5	5	5	5
Sulphur	2	2	2	2	2	2	2
Resorcinol	–	–	–	2.5	–	2.5	2.5
Silica†	–	–	–	–	5	5	5
Stearic acid	2	2	2	2	2	2	2
Silk‡	–	10	20	20	20	20	–
Hexamine§	–	–	–	1.6	–	1.6	1.6
CBS¶	0.8	0.8	0.8	0.8	0.8	0.8	0.8

*Nitrile rubber, PERBUNAN N 3307 NS, supplied by Bayer Ltd., West Germany.
†Vulcasil-S, precipitated reinforcing silica, supplied by Bata India Ltd., Calcutta.
‡Silk fibre (*Mulberry type*), obtained as waste in filatures of Silk Khadi Mondol, Bishnupur, West Bengal.
§Hexamethylenetetramine, supplied by May and Baker, England.
¶N-cyclohexyl 2-benzothiazole sulfenamide, obtained from the Alkali and Chemical Corp. of India Ltd., Rishra.

TABLE II Characterization of the vulcanizates A to G

Property	Fibre orientation*	Vulcanizate						
		A	B	C	D	E	F	G
Optimum cure time at 150° C (min)	–	16.0	15.0	12.0	8.5	15.0	11.0	11.0
Hardness, Shore A	–	57	85	93	85	92	90	61
Tear strength ($kN\,m^{-1}$)	L	16.6	25.2	30.2	36.6	45.1	49.2	22.3
	T		22.5	26.3	36.0	44.0	55.9	
Tensile strength (MPa)	L	2.11	3.67	4.08	4.40	4.19	7.99	8.54
	T		2.69	3.37	4.47	3.41	5.22	
Elongation at break (%)	L	450	45	50	80	17	20	550
	T		115	60	240	100	485	
Modulus at 100% elongation (MPa)	L	1.14	–	–	–	–	–	1.33
	T		2.65	–	3.45	3.41	4.56	
Modulus at 25% elongation (MPa)	L	0.52	2.95	4.69	4.19	–	–	0.73
	T		1.80	3.93	2.15	3.59	2.67	
Heat build-up for 10 min (ΔT) at 50° C (° C)†	L	16	25 (7)	29 (4)	26 (5)	40 (8)	30	20
	T		26 (6)	31 (3)	28 (4.5)	44 (7)	33	
V_r	–	0.140	0.135	0.138	0.146	0.103	0.192	0.145

*L denotes longitudinal and T denotes transverse orientation.
†Values in the bracket indicate time (min) of failure of the samples.

From Table II, it is also evident that when adhesion between the fibre and the rubber matrix was not good (e.g. for the mixes B, C, D and E), the test specimens in the Goodrich flexometer could not withstand dynamic compression and failed at a much earlier stage than scheduled. When proper bonding occurred between the fibre and the matrix (mix F), the sample did not fail and showed less heat build-up too. Presence of unbonded loose fibres in the mixes B, C, D and E make these composites very susceptible to vibration failure, thereby showing higher heat build-up. Higher heat generation in samples with transversely oriented fibres unlike in the samples with longitudinally oriented fibres is in agreement with our earlier studies [1].

Comparison of the properties for mix F and mix G (containing the ingredients in the same proportions as in mix F, except the fibre) show that although there is a slight drop in tensile strength and increase in heat build-up in mix F, the improvement in tear strength, modulus and hardness is excellent. Anisotropy in stress–strain properties (Figs. 3a and b) is prominent for mix F and the restriction to solvent swelling (V_r values) is also maximum in mix F. The V_r values can be taken as a measure of the reinforcing ability of the fillers [23, 24]. These observations indicate that fibre reinforcement in nitrile rubber composites takes place when all the components of the bonding agents e.g. silica, resorcinol and hexamine, are present together. The fibre reinforced vulcanizates show much improvement in most of the properties with marginal losses in a few.

3.2. Determination of the optimum concentration of bonding agents *vis-à-vis* fibre loading

Formulations of the mixes are given in Table III and the corresponding vulcanizate characteristics in Table IV. At fixed concentrations of resorcinol–hexamine and fibre, the role of silica in adhesion has been studied first. Comparison of the tensile strength, elongation at break and V_r values for the mixes F, H and I show that as the concentration of silica increases from 5 phr to 20 phr the adhesion between the fibre and the matrix progressively decreases, and at 20 phr silica (mix I) the composite behaves more like a silica reinforced rubber than a fibre reinforced rubber. This is evident from its very high elongation and low tensile strength as compared to mixes F and H, and also from the

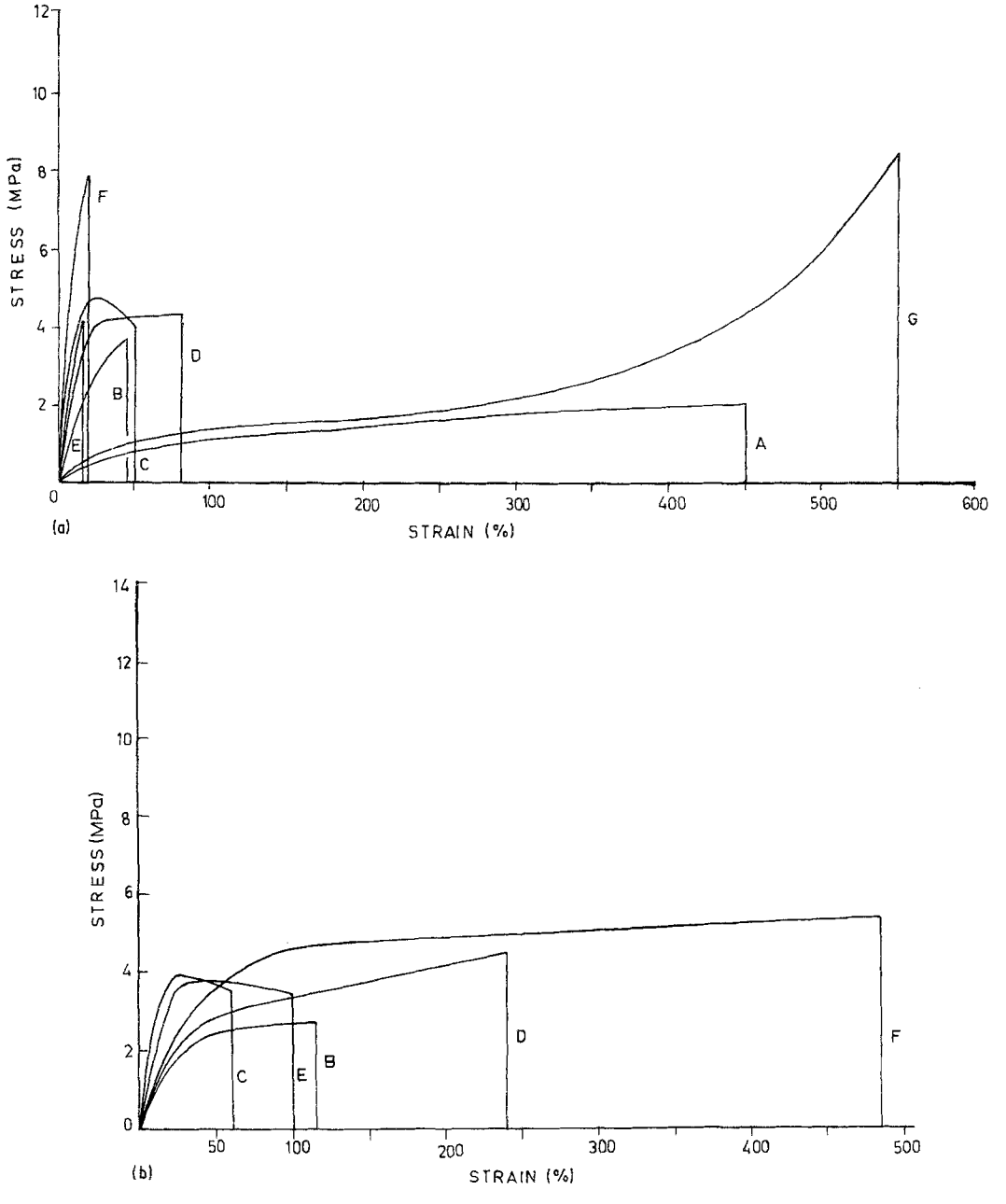

Figure 3 (a) Stress–strain curves of mixes A, B, C, D, E, F and G; fibres oriented along the grain direction (mixes B, C, D, E and F). (b) Stress–strain curves of mixes B, C, D, E and F; fibres oriented across the grain direction.

fact that its properties are very similar to that of mix J (without fibre). Tensile strength for the mix I is less than that of mix J because the presence of unbonded fibres in the former weakens the matrix by creating more flaws which act as the centres of initiation of a ready tensile rupture.

Next, the effect of different proportions of resorcinol, hexamine and silica on the composite properties at a particular fibre loading (20 phr), was studied (mixes K and L). Comparison of the strength properties, V_r values and analyses of stress–strain data (Figs. 4a and b) shows that 10 phr of silica, 5 phr of resorcinol and 3.2 phr of hexamine (as in mix L) are needed for 20 phr fibre loading for maximum reinforcement. In order to confirm this observation, mixes with 10 phr fibre

TABLE III Formulations of the mixes H to O

Ingredient	Content of mix (parts by weight)							
	H	I	J	K	L	M	N	O
NBR	100	100	100	100	100	100	100	100
Zinc oxide	5	5	5	5	5	5	5	5
Sulphur	2	2	2	2	2	2	2	2
Resorcinol	2.50	2.50	2.50	5.00	5.00	2.50	1.25	1.25
Silica	10	20	20	5	10	5	5	2.5
Stearic acid	2	2	2	2	2	2	2	2
Silk	20	20	–	20	20	10	10	10
Hexamine	1.6	1.6	1.6	3.2	3.2	1.6	0.8	0.8
CBS	0.8	0.8	0.8	0.8	0.8	0.8	0.8	0.8

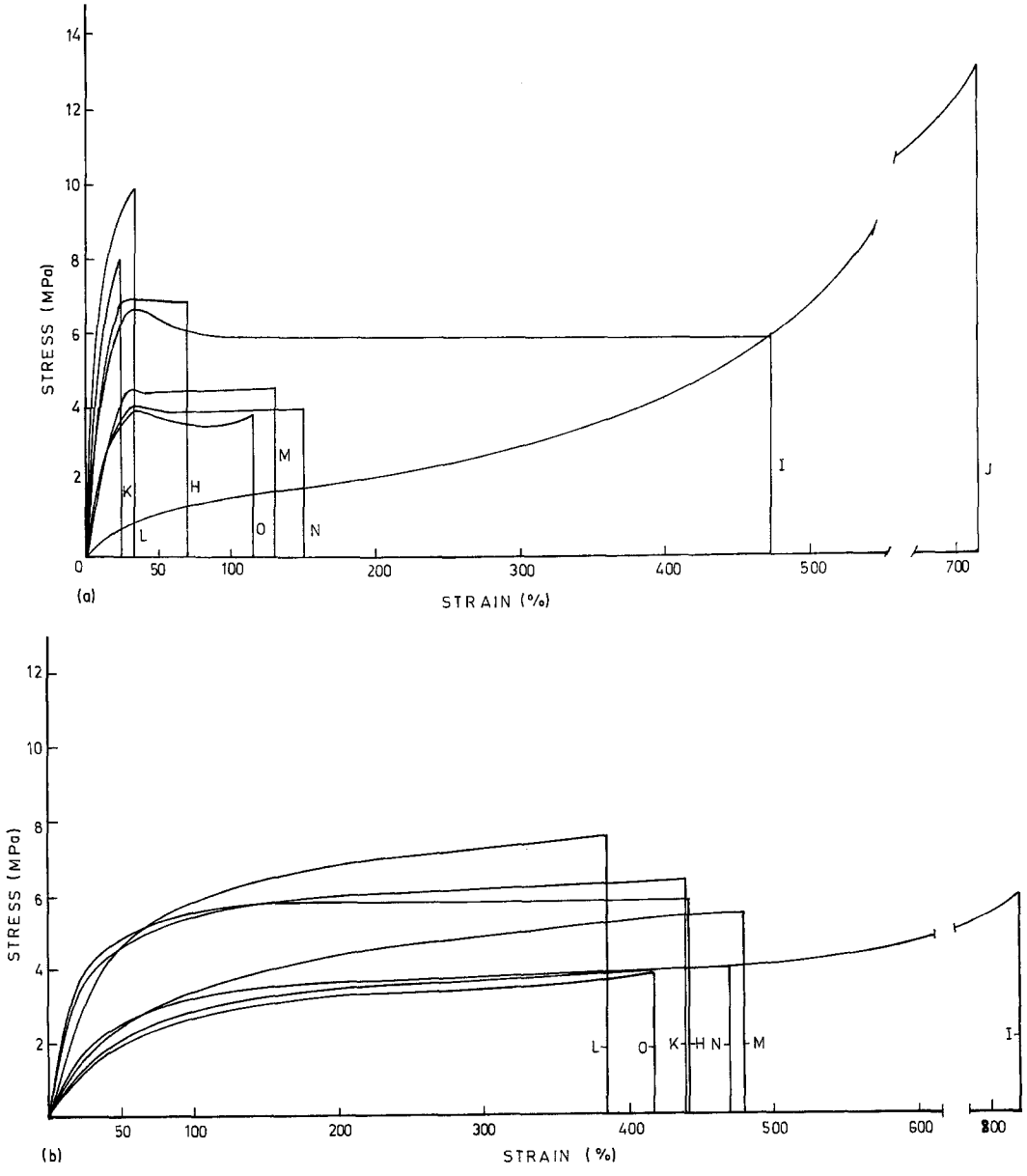

Figure 4 (a) Stress–strain curves of mixes H, I, J, K, L, M, N and O; fibres oriented along the grain direction (mixes H, I, K, L, M, N and O). (b) Stress–strain curves of mixes H, I, K, L, M, N and O; fibres oriented across the grain direction.

TABLE IV Characterization of the vulcanizates H to O

Property	Fibre orientation	Vulcanizate							
		H	I	J	K	L	M	N	O
Optimum cure time at 150° C (min)	–	12.75	14.25	12.50	9.50	10.50	11.25	12.50	11.75
Hardness, Shore A	–	93	87	70	94	95	85	84	83
Tear strength ($kN\,m^{-1}$)	L	49.5	62.4	33.9	52.9	57.9	39.2	38.6	34.9
	T	55.3	47.8		50.8	65.8	47.1	44.3	35.0
Tensile strength (MPa)	L	6.79	5.86	13.06	8.06	9.80	4.47	3.91	3.72
	T	5.87	6.40		6.41	7.54	5.52	4.04	3.85
Elongation at break (%)	L	70	473	715	24	32	130	150	115
	T	442	820		440	385	480	470	418
Modulus at 100% elongation (MPa)	L	–	5.82	1.57	–	–	4.43	3.81	3.46
	T	5.67	3.24		5.54	5.85	3.31	2.83	2.58
Modulus at 25% elongation (MPa)	L	6.87	6.50	0.95	–	9.61	4.22	3.88	3.81
	T	4.17	1.90		3.89	3.26	1.57	1.50	1.37
Heat build-up for 10 min (ΔT) at 50° C (° C)	L	34	38	29	31	34	28	32	30
	T	39	46		33	38	30	33	32
V_r	–	0.185	0.109	0.136	0.238	0.235	0.140	0.125	0.136

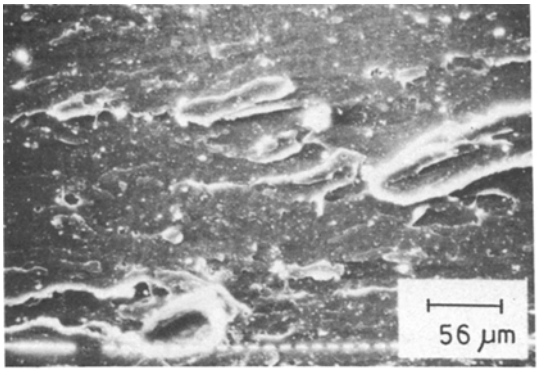

Figure 5 SEM photomicrograph of the tensile fractured surface of mix G.

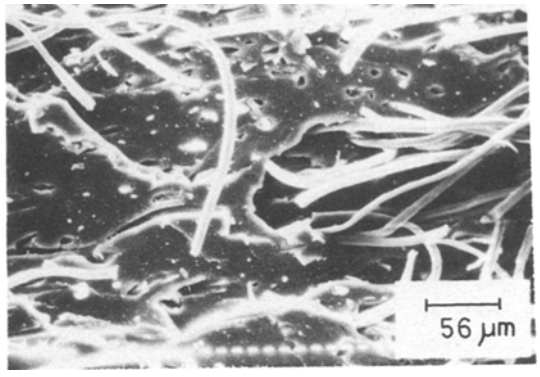

Figure 7 SEM photomicrograph of the tensile fractured surface of mix C; fibres oriented along the grain direction.

loading (mixes M, N and O) and different proportions of the bonding agents were taken. From the improvement in properties of mix M (containing 5 phr silica, 2.5 phr resorcinol and 1.6 phr hexamine), it was clear that the optimum proportion of the bonding agents was the same as that found earlier for mix L. Mixes L and M are, therefore, considered to consist of requisite proportions of bonding agents for 20 phr and 10 phr fibre, respectively.

Fig. 5 is the SEM photomicrograph of a tensile fractured surface of mix G (without fibre). A rough surface due to chunking of materials is observable. Addition of fibre changes the failure mode. Fig. 6 is the SEM photomicrograph of a tensile fractured surface of mix L with longitudinal fibre orientation. Proper adhesion between the fibre and the matrix causes less pulling out and, therefore, less pitting on the surface and a higher extent of breakage of the fibres. Fig. 7, which is the SEM photomicrograph of a tensile fractured surface of mix C with longitudinal fibre orientation, shows greater pulling out of the fibre, more pit formation on the surface and less fibre breakage as compared to Fig. 6. This observation is in agreement with the results of tensile strength for the mix C compared to mix L.

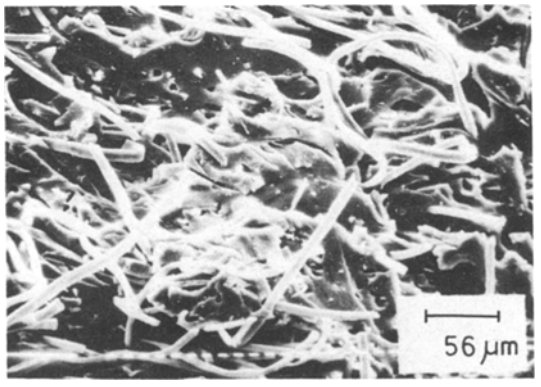

Figure 6 SEM photomicrograph of the tensile fractured surface of mix L; fibres oriented along the grain direction.

3.3. Effect of fibre concentration on composite properties

Table V gives the formulations of the mixes P, Q, M, R, L and S and the characterization of the vulcanizates is given in Table VI. Here we have studied the effect of fibre concentration on the properties of the composite containing the optimum level of silica, resorcinol and hexamine. Figs. 8a and b shows the stress–strain curves of the mixes.

Tensile strength of the composite with either longitudinal or transverse orientations of the fibre increases with the increase in fibre loading up to 20 phr beyond which it remains almost constant. A higher tensile strength of composites with longitudinal orientation than those with transverse orientation of fibres is always observed. This is because greater hindrance to the progress of fracture front is experienced when fibres are oriented longitudinally (i.e. perpendicular to the fracture direction). Breakage and pulling out of the fibres take place mainly when fibres are oriented in the longitudinal direction whereas for transversely oriented fibres the crack progresses in the direction of fibre alignment. Tensile strength of composites with longitudinal fibre orientation is, therefore, always higher than those with transverse fibre orientation. This observation is similar to the earlier results [1, 5, 8, 10, 25]. Lower tensile strength of the composites from mixes Q, M, R, L and S than that of mix P (containing no fibre) may be due to

TABLE V Formulations of the mixes P to S

Ingredient	Content of mix (parts by weight)					
	P	Q	M	R	L	S
NBR	100	100	100	100	100	100
Zinc oxide	5	5	5	5	5	5
Sulphur	2	2	2	2	2	2
Resorcinol	5.00	1.25	2.50	3.75	5.00	6.25
Silica	10.0	2.5	5.0	7.5	10.0	12.5
Stearic acid	2	2	2	2	2	2
Silk	–	5	10	15	20	25
Hexamine	3.2	0.8	1.6	2.4	3.2	4.0
CBS	0.8	0.8	0.8	0.8	0.8	0.8

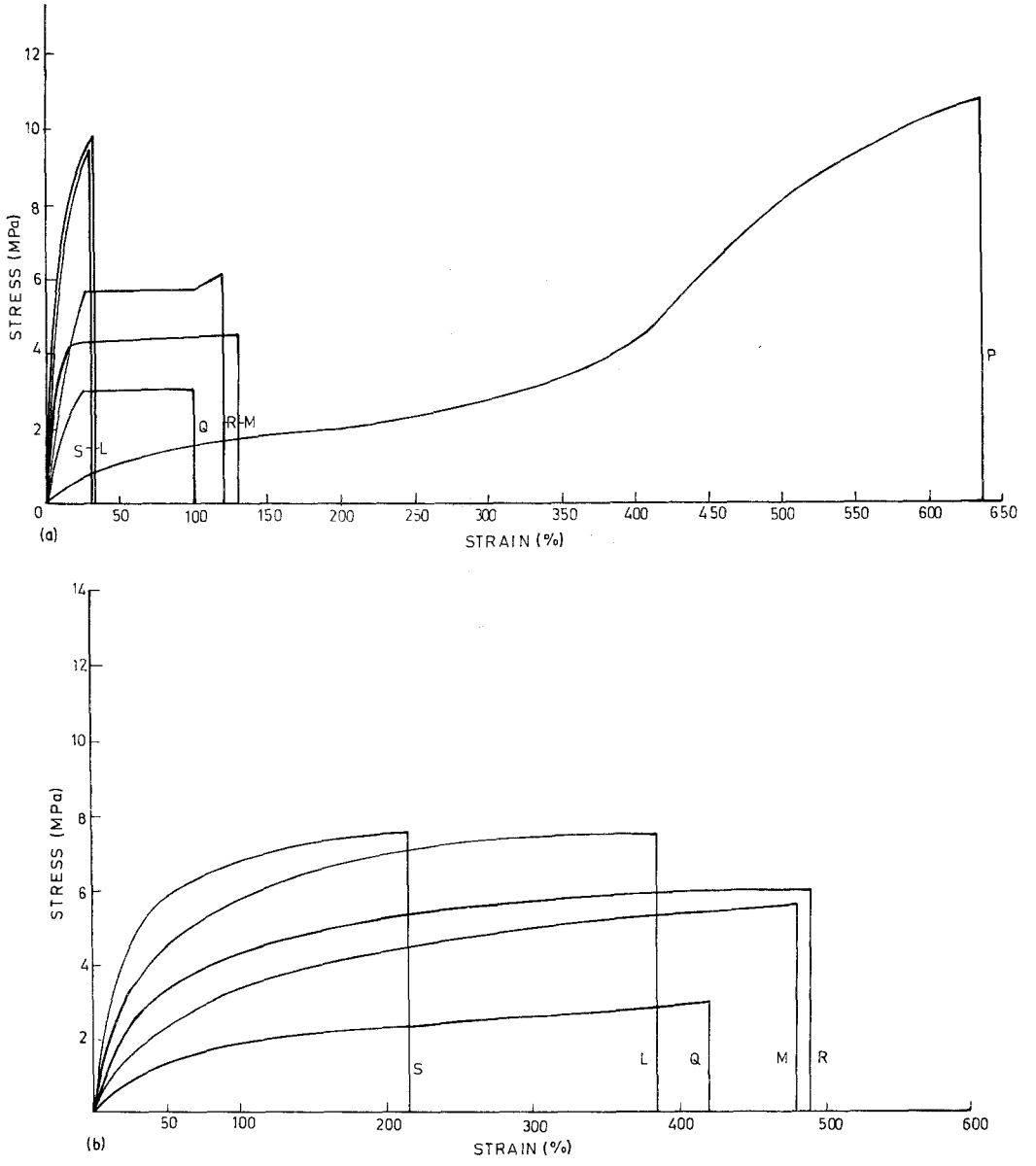

Figure 8 (a) Stress–strain curves of mixes P, Q, M, R, L and S; fibres oriented along the grain direction (mixes Q, M, R, L and S). (b) Stress–strain curves of mixes Q, M, R, L and S; fibres oriented across the grain direction.

TABLE VI Characterization of the vulcanizates P to S

Property	Fibre orientation	Vulcanizate					
		P	Q	M	R	L	S
Optimum cure time at 150° C (min)	–	10.50	12.00	11.25	10.00	10.50	9.50
Hardness, Shore A	–	66	78	85	92	95	98
Tear strength (kN m^{-1})	L	28.4	20.0	39.2	44.3	57.9	63.9
	T		27.2	47.1	55.8	65.8	58.9
Tensile strength (MPa)	L	10.74	3.06	4.47	6.08	9.80	9.55
	T		2.94	5.52	5.94	7.54	7.41
Elongation at break (%)	L	635	100	130	120	32	30
	T		420	480	490	385	215
Modulus at 100% elongation (MPa)	L	1.43	3.06	4.43	5.70	–	–
	T		1.80	3.31	4.36	5.85	6.94
Modulus at 25% elongation (MPa)	L	0.76	3.02	4.22	5.65	9.61	8.91
	T		0.95	1.57	2.41	3.26	4.73
Heat build-up for 10 min (ΔT) at 50° C (° C)	L	22	24	28	31	34	36
	T		25	30	34	38	42
Compression set at constant strain (25%) (%)	L	58	64	66	68	70	73
	T		60	63	64	66	71
Compression set at constant stress of 400 lb (%)	L	20	19	12	11	9	8
	T		20	14	12	11	10
Resilience (%)	–	57	56	53	49	47	43
Abrasion loss (cc h^{-1})	L	0.86	0.71	1.09	1.17	1.26	1.34
	T		0.67	0.88	1.05	1.11	1.24
V_r	–	0.147	0.139	0.140	0.208	0.235	0.250

the fact that optimum cure at a temperature of 150° C does not produce adhesion to its fullest extent, and the presence of loose fibres, causes easy failure of the matrix. The adhesion level is improved considerably on slow post curing of the composites and this is reflected in the per cent retention of properties of the composites after ageing. Ageing leads to the deterioration of properties of the non-fibre filled mix P (without fibre) but with a simultaneous improvement of the composite properties supporting the above observation (Table IX).

V_r values, given in Table VI, show that beyond a fibre loading of 15 phr, a pronounced restriction to swelling in chloroform takes place. This result, therefore, is in agreement with the above conclusion that adhesion between fibre and rubber takes place to a significant extent only beyond a loading of 15 phr of fibre.

Significant improvement in tear strength has been observed when fibres are present in the mixes. Tear strength increases with increasing fibre concentration in the mixes. Up to 20 phr fibre loading the tear strength increases to a lesser extent when fibres are oriented longitudinally than when they are oriented transversely. Beyond 20 phr loading of the fibre the tear strength drops in the case of transverse orientation and thus the anisotropic effect in tear strength becomes evident. With longitudinal orientation, tear strength is dependent on the extent of obstruction to the tear path propagating perpendicularly which, in turn, is proportional to the fibre concentration. When the obstruction is sufficient (namely, at 20 phr fibre level) the tear strength for the composite may be considered equal to the sum total of the tear strength of the bare matrix and the obstruction produced by the fibres. When the obstruction is not sufficient (namely, for the mix M with 10 phr fibre) this relation does not hold good. Tear strength values for some mixes are given in Table VII in order to confirm the above view.

In the case of transverse orientation of fibres, most of the fibres are oriented parallel to the direc-

TABLE VII Tear strength of composites with longitudinally oriented fibres

Vulcanizate	Tear strength observed ($kN\,m^{-1}$)	Theoretical value ($kN\,m^{-1}$)
I	62.4	Sum of tear strength values for the mixes J and C = 33.9 + 30.2 = 64.1
L	57.9	Sum of tear strength values for the mixes P and C = 28.4 + 30.2 = 58.6
M	39.2	Sum of tear strength values for the mixes G and B = 22.3 + 25.2 = 47.5

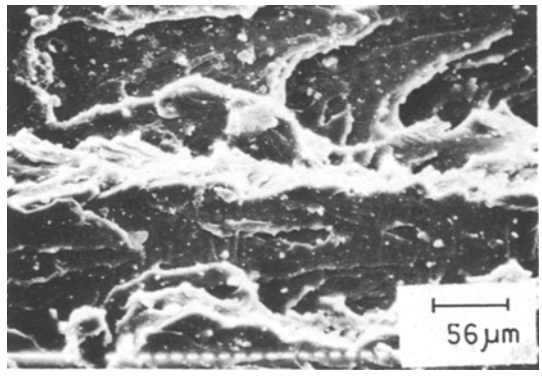

Figure 9 SEM photomicrograph of the tear fractured surface of mix P.

tion of crack propagation and thus offer less resistance to the propagating tear. Hence the additive equation does not apply here. For the mixes with transversely oriented fibres, the fibres and matrix constitute one system and the tear strength depends on the tearing energy of the composites. Tearing energy may be calculated from the area under the curves obtained in the force–tear chart of the Instron Universal Testing Machine. Areas under the curves (Table VIII) follow the order; $P > Q_T < M_T < R_T < L_T > S_T$, which is the same as the observed tear strength values.

Fig. 9 is the SEM photomicrograph of tear fractured surface of mix P (without fibre). Shear fracture in different planes and tear paths are observable. Addition of fibre changes the fracture mode.

Fig. 10 is the SEM photomicrograph of tear fractured surface of mix L with longitudinal fibre orientation. Absence of pulling out of the fibres and consequent greater hindrance to the smooth progress of the tear accounts for a higher tear strength of the mix with longitudinal orientation of fibres. Fig. 11 is the SEM photomicrograph of tear fractured surface of mix C (longitudinal fibre orientation). Insufficient adhesion between fibres and the matrix causes pulling out of the fibres which leads to the creation of holes on the surface. Thus the resistance to tearing is small and the mix C shows lower tear strength than mix L.

It has been observed that tearing in composites with transverse orientation of fibres does not depend on the obstruction due to fibres, which can be easily visualized from the SEM photomicrograph (Fig. 12) of tear fractured surface of mix M (with transversely oriented fibres). Orientation of the fibres parallel to fracture propagation and presence of cracks on the surface accounts for poor tear strength of this mix.

Elongation at break for the mixes with longitudinally oriented fibres drops drastically with the addition of fibres up to a loading of 20 phr, beyond which it remains almost constant. In the case of transverse orientation of fibres a gradual decreasing trend is observed, although higher values for elongation at break in this orientation as compared to the corresponding values in the case of longitudinal orientation of the fibres are always obtained.

Modular anisotropy both at 25% and 100%

TABLE VIII Tear strength of composites with transversely oriented fibres

Vulcanizate	Fibre concentration (phr)	Observed tear strength ($kN\,m^{-1}$)	Estimated area from Instron force–tear chart (arbitrary unit)
P	0	28.4	1577
Q	5	27.2	1504
M	10	47.1	2695
R	15	55.8	3112
L	20	65.8	3733
S	25	58.9	3387

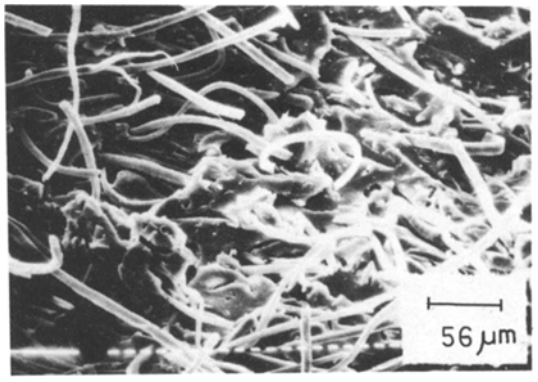

Figure 10 SEM photomicrograph of the tear fractured surface of mix L; fibres oriented along the grain direction.

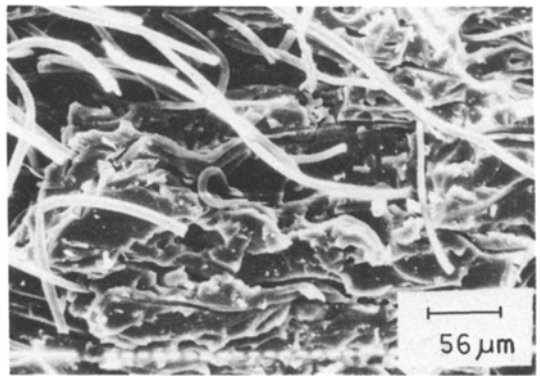

Figure 12 SEM photomicrograph of the tear fractured surface of mix M; fibres oriented across the grain direction.

elongation for the mixes are given in Table VI. Higher modulus for the fibre filled mixes as compared to the unfilled one (mix P) are always observed. Both 25% and 100% modulus increase with increase in fibre loading although higher values are always observed in the case of longitudinal orientation of fibres in the mixes.

Continuous increase in hardness and decrease in resilience was observed with the increase of fibre concentration in the mixes.

Compression set has been determined at constant stress and at constant strain. Stiffness of the vulcanizates increases with increase in fibre content. It is also expected that stiffness of the sample with longitudinally oriented fibres will be higher as compared to that for the transversely oriented ones. This is reflected in the properties obtained for both types of set. Compression set at constant stress for both orientations decreases as the concentration of fibres increases because of the increasing stiffness of the composites. Lower values of compression set for longitudinal orientation of fibres as compared to that for the transverse orientation are in agreement with our above explanation. In the case of compression set at constant strain, however, the result of compression set, is just the opposite. Here increasing stiffness requires increasing applied load for the same strain (25%) causing an increase in compression set with the increase in fibre loading and higher values in the case of longitudinally oriented fibres than that for transversely oriented fibres.

Abrasion loss varies with the variation of fibre concentration in the composites. Abrasion resistance for the composites has been measured for two types of orientations:

(a) Orientation of the fibres in the test specimens such that they experience a frictioning force parallel to the direction of sliding of the abrading surface. This is denoted as longitudinal (L) orientation.

(b) Orientation of the fibres across the above arrangement, such that they experience a frictional force perpendicular to the direction of sliding of the abrading surface. This is denoted as transverse (T) orientation. Abrasion loss is mainly due to loss of fibres. Increase in abrasion loss with the increase in fibre loading is less than expected owing to enhanced fibre–rubber adhesion. Abrasion loss for longitudinal orientation is more compared to that for transverse orientation. This observation is in agreement with the observation of other workers [26, 27] who have suggested that the extra work necessary to bend and break the fibres is responsible for the higher wear resistance exhibited by composites with fibres oriented perpendicular to the counterface as compared to those with fibres oriented parallel to the sliding surface.

Fig. 13 is the SEM photomicrograph of the

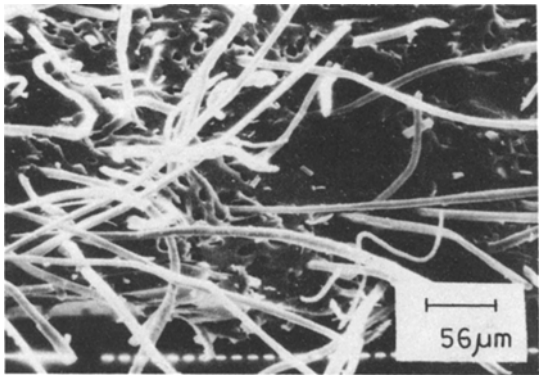

Figure 11 SEM photomicrograph of the tear fractured surface of mix C; fibres oriented along the grain direction.

TABLE IX Ageing properties of the mixes (Per cent retention of properties after ageing for 48 h at 100° C)

Property	Fibre orientation	Vulcanizate					
		P	Q	M	R	L	S
Tensile strength	L	69	113	125	148	160	155
	T		99	107	124	147	135
Elongation at break	L	45	87	74	73	66	67
	T		52	50	45	36	46
Tear strength	L	77	95	89	92	89	80
	T		80	75	79	72	68

abraded surface of mix P (without fibre). Material displacement and cavitation occur on the fracture surface. Addition of fibre changes the abraded surface. Fig. 14 is the SEM photomicrograph of the abraded surface of mix L with longitudinally oriented fibres. It shows fibres oriented parallel to the sliding surface. In the transverse orientation (Fig. 15), bending of fibres is evident. This is consistent with our discussion in the preceding paragraphs.

Stiffness of the composites increases with increase in fibre loading. Increased stiffness requires application of higher mechanical stress to maintain constant strain in the samples in Goodrich flexometer testing. Heat build-up for both longitudinal and transverse orientations of the fibre, therefore, increases with increase in fibre concentration. In the transverse orientation, however, number of pulled out fibres and consequent frictioning among them increases with the increase in fibre concentration. The higher rate of temperature rise with respect to fibre loading is, therefore, observed in composites with transverse orientation of fibres as compared to those with longitudinal orientation of fibres.

Figs. 16 and 17 are the SEM photomicrographs of the failed surface of the Goodrich flexometer test specimen of mix P (without fibre). Characteristics of fatigue failure along with nodular cavitation are observable. Addition of fibre changes the failure mode. Fig. 18 is the SEM photomicrograph of the failed surface of Goodrich flexometer test specimen of mix L with longitudinal fibre orientation. Absence of both pulling out and breakage of fibres and deformation of fibres along with the matrix are observed. In the case of transversely oriented fibres in the same mix L (Fig. 19) matrix deformation is less and the fibres undergo breakage and are pulled out from the surface. Frictioning among these free ends leads to higher heat generation. Formation of pits due to pulling out of the fibres are also observed in Fig. 19.

3.4. Effect of ageing on fibre–matrix adhesion

Per cent retention of properties after ageing for 48 h at 100° C for the mixes is given in Table IX.

Percentage retention of tensile strength, tear strength and elongation at break after ageing for the properly bonded fibre-filled mixes is more as compared to the mix P (without fibre). This result is in agreement with our earlier studies [1, 10]. Unlike the fibres, the matrix gets deteriorated on ageing and there is an expected fall in the strength

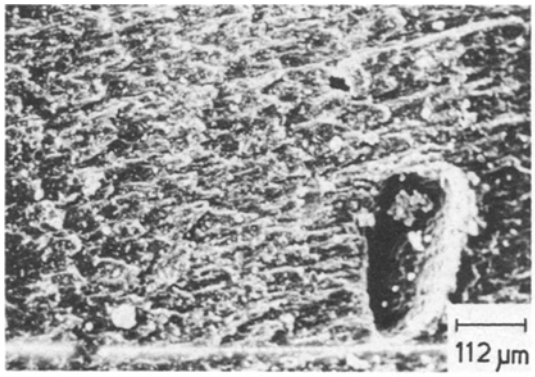

Figure 13 SEM photomicrograph of the abraded surface of mix P.

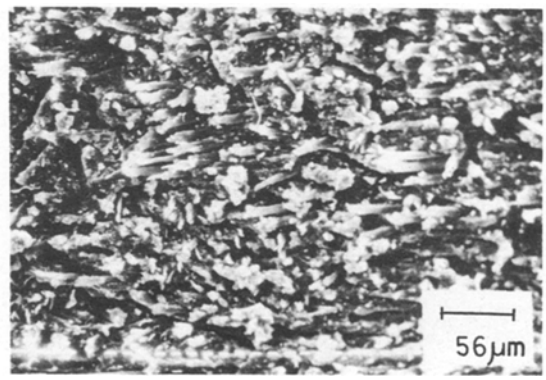

Figure 14 SEM photomicrograph of the abraded surface of mix L; fibres oriented along the sliding direction.

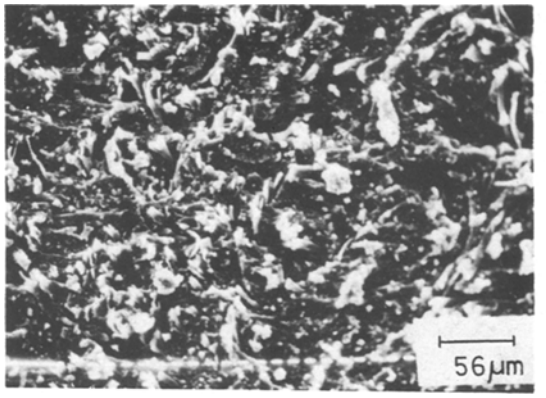

Figure 15 SEM photomicrograph of the abraded surface of mix L; fibres oriented across the sliding direction.

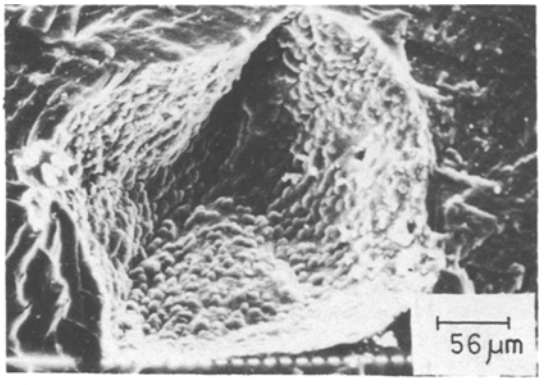

Figure 17 SEM photomicrograph of the failed surface of the Goodrich flexometer test specimen of mix P.

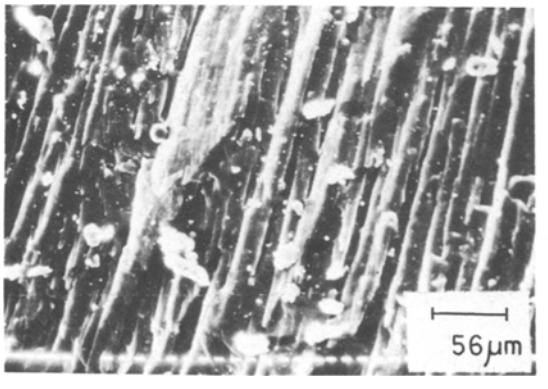

Figure 16 SEM photomicrograph of the failed surface of the Goodrich flexometer test specimen of mix P.

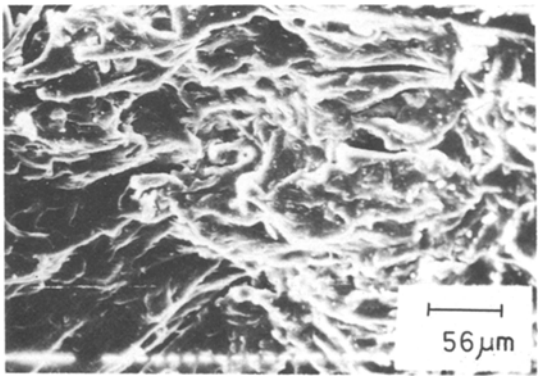

Figure 18 SEM photomicrograph of the failed surface of the Goodrich flexometer test specimen of mix L; fibres oriented along the direction of applied load.

properties. However, improvement in the adhesion level between the fibre and the matrix checks the effect of the matrix deterioration and accounts for the higher retention of strength properties.

3.5. Processing characteristics

The presence of fibres in the mixes affects the processing characteristics signficiantly as shown in Table X. Green strength of the compounds with either longitudinal or transverse orientations of fibres increases with increase in fibre concentration. However, the increase is less pronounced in the case of transverse orientation. Significant

TABLE X Processing characteristics of the mixes

Property	Fibre orientation	Vulcanizate		
		P (No fibre)	M (10 phr fibre)	L (20 phr fibre)
Green strength (MPa)	L	0.22	1.45	2.61
	T		0.67	0.82
Mill shrinkage (%)	–	10	2	1
Elongation at break (%)	L	150	70	50
	T		120	90
Mooney viscosity ML(1 + 4), at 120° C	–	33.0	38.0	44.5
Mooney scorch time, T_5 at 120° C (min)	–	18.5	22.0	24.0

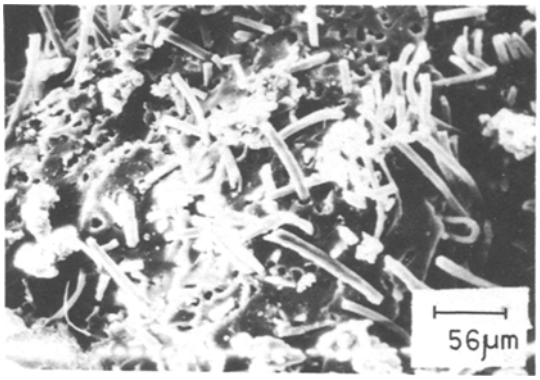

Figure 19 SEM photomicrograph of the failed surface of the Goodrich flexometer test specimen of mix L; fibres oriented across the direction of applied load.

improvement in mill shrinkage is also observed with increase in fibre concentration in the mixes. Values of the elongation at break for the green compounds follow the expected decrease with increase in fibre loading and consistently higher values are observed in the case of transverse fibre orientation as compared to those in the longitudinal orientation. Mooney viscosity increases continuously with fibre loading. Increase in fibre concentration increases the Mooney scorch time. This may be due to the presence of acidic (carboxyl) groups in the fibre. Improvement in the processing characteristics for silk fibre-nitrile rubber compounds is similar to the results of earlier studies [1, 9, 10].

Acknowledgement

Thanks are due to the National Council of Educational Research and Training, New Delhi, for financial assistance.

References

1. D. K. SETUA and S. K. DE, *Rubber Chem. Technol.* (in press).
2. J. M. CAMPBELL, *Prog. Rubber Technol.* **41** (1978) 43.
3. A. Y. CORAN, P. HAMED and L. A. GOETTLER, *Rubber Chem. Technol.* **49** (1976) 1167.
4. K. BOUSTANY and R. L. ARNOLD, *J. Elastoplast.* 8 (1976) 160.
5. J. E. O'CONNOR, *Rubber Chem. Technol.* **50** (1977) 945.
6. S. R. MOGHE, Paper presented at the Symposium of Rubber Division on Cord/Rubber Composites, ACS, Chicago (October 1982).
7. K. BOUSTANY and A. Y. CORAN, US Patent No. 3697364 (October 1972).
8. V. M. MURTY and S. K. DE, *Rubber Chem. Technol.* **55** (1982) 287.
9. V. M. MURTY and S. K. DE, *J. Appl. Polym. Sci.* in press.
10. S. K. CHAKRABORTY, D. K. SETUA and S. K. DE, *Rubber Chem. Technol.* **55** (1982) 1286.
11. J. R. CREASEY and M. P. WAGNER, *Rubber Age* **100** (1968) 72.
12. N. L. HEWITT, *ibid.* **104** (1972) 59.
13. E. MORITA, *Rubber Chem. Technol.* **53** (1980) 795.
14. L. A. GOETTLER, R. I. LIEB and A. J. LAMBRIGHT, *ibid.* **52** (1979) 838.
15. J. R. BEATTY and P. HAMED, Paper presented at the Meeting of Rubber Chemistry Division, ACS, Montreal, Quebec, Canada (may 1978) in press.
16. J. W. ROGERS and D. W. CARLSON, Paper presented at the Meeting of Rubber Division, ACS, Minneapolis, Minnesota (April 1976) in press.
17. L. A. GOETTLER, R. I. LIEB, P. J. DIMAURO and K. E. KEAR, Paper presented at the fall Technical Seminar of the Detroit Rubber Group (October 1979) in press.
18. J. W. HORVATH, Paper presented at the Meeting of Rubber Division, ACS, Atlanta, GA (March 1979) in press.
19. D. K. SETUA and S. K. DE, *J. Mater. Sci.* **18** (1983) 847.
20. B. ELLIS and G. N. WELDING, "Techniques of Polymer Science" (Society for Chemical Industry, London, 1964) p. 46.
21. *Idem, Rubber. Chem. Technol.* **37** (1964) 571.
22. A. P. FOLDI, *ibid.* **49** (1976) 379.
23. B. DAS, *J. Appl. Polym. Sci.* **17** (1973) 1019.
24. S. K. CHAKRABORTY and S. K. DE, *ibid.* **27** (1982) 4561.
25. G. C. DERRINGER, *Rubber World* **165** (1975) 45.
26. Z. ELIEZER, V. D. KHANNA and M. F. AMATENU, *Wear* **53** (1979) 387.
27. NAK-HO SUNG and NAM P. SUH, *ibid.* **53** (1979) 129.

Received 26 April
and accepted 21 July 1983